Molecular Microbiology (2009) 72(4), 1068–1079 ■
doi:10.1111/j.1365-2958.2009.06713.x
First published online 30 April 2009

Perturbation of phosphatidylethanolamine synthesis affects mitochondrial morphology and cell-cycle progression in procyclic-form *Trypanosoma brucei*

Aita Signorell,[1†‡] Eva Gluenz,[2‡] Jochen Rettig,[3] André Schneider,[3] Michael K. Shaw,[2] Keith Gull[2] and Peter Bütikofer[1*]

[1]*Institute of Biochemistry & Molecular Medicine and* [3]*Department of Chemistry & Biochemistry, University of Bern, 3012 Bern, Switzerland.*

[2]*Sir William Dunn School of Pathology, University of Oxford, Oxford OX1 3RE, UK.*

Summary

Phosphatidylethanolamine (PE) and phosphatidylcholine (PC) are the two major constituents of eukaryotic cell membranes. In the protist *Trypanosoma brucei*, PE and PC are synthesized exclusively via the Kennedy pathway. To determine which organelles or processes are most sensitive to a disruption of normal phospholipid levels, the cellular consequences of a decrease in the levels of PE or PC, respectively, were studied following RNAi knock-down of four enzymes of the Kennedy pathway. RNAi against ethanolamine-phosphate cytidylyltransferase (ET) disrupted mitochondrial morphology and ultrastructure. Electron microscopy revealed alterations of inner mitochondrial membrane morphology, defined by a loss of disk-like cristae. Despite the structural changes in the mitochondrion, the cells maintained oxidative phosphorylation. Our results indicate that the inner membrane morphology of *T. brucei* procyclic forms is highly sensitive to a decrease of PE levels, as a change in the ultrastructure of the mitochondrion is the earliest phenotype observed after RNAi knock-down of ET. Interference with phospholipid synthesis also impaired normal cell-cycle progression. ET RNAi led to an accumulation of multinucleate cells. In contrast, RNAi against choline-/ethanolamine phosphotransferase, which affected PC as well as PE levels, caused a cell division phenotype characterized by non-division of the nucleus and production of zoids.

Accepted 18 April, 2009. *For correspondence. E-mail peter.buetikofer@mci.unibe.ch; Tel. (+41) 31 631 4113; Fax (+41) 31 631 3737. †Present address: Department of Biochemistry, Weill Cornell Medical College, New York, NY 10065, USA. ‡These authors contributed equally to this work.

Introduction

Cellular membranes are complex mixtures of lipids and proteins and maintaining the specific composition of the plasma and organellar membranes is a dynamic, tightly regulated process fundamental to the survival and proliferation of a cell. Lipid and protein compositions vary between organisms, cell types and subcellular organelles and between the two leaflets of the lipid bilayer (van Meer *et al.*, 2008). Membrane lipid composition and turnover not only affects cell and organelle biogenesis, but also membrane and protein function. It has been well established that modulation of, for example, phosphatidylethanolamine (PE) and cardiolipin concentrations in bacterial and mitochondrial membranes, and in many model membrane systems, may result in misfolding or topological misorientation of membrane proteins resulting in dysfunctional proteins (Bogdanov and Dowhan, 1999; Jensen and Mouritsen, 2004; Lee, 2004; Mileykovskaya *et al.*, 2005). Membrane lipid abnormalities have also been implicated in several diseases, many of them affecting mitochondrial membrane and protein function (Bogdanov *et al.*, 2008).

The complex tubular network of the single mitochondrion in *Trypanosoma brucei* parasites represents an extreme form within a spectrum of diverse mitochondrial structures across eukaryotes (Schneider, 2001; Embley and Martin, 2006). It is subject to morphological and functional changes during differentiation between the distinct life-cycle stages. Mitochondria in slender bloodstream parasites in the mammalian host form a single tube with few short cristae and there is no functional Krebs cycle. During the slender-to-stumpy transformation, a respiratory switch occurs whereby the mitochondrion develops well-defined tubular cristae and becomes active in NADH oxidation (Vickerman, 1965; Brown *et al.*, 1973). Transformation from stumpy bloodstream forms to procyclic trypanosomes is accompanied by a switch from glucose oxidation to proline oxidation. In procyclic forms, which proliferate in the tsetse fly midgut, a fully functional Krebs

cycle operates and the mitochondrion forms an extensive tubular network with plate-like cristae (Brown *et al*., 1973). Clearly, mitochondrial structure is dynamic and there are correlations between structure and function where protein and lipid compositions are critical determinants. However, the regulatory mechanisms of mitochondrial morphogenesis are not understood.

In *T. brucei*, PE and phosphatidylcholine (PC) together comprise about 70% of total membrane phospholipids (Patnaik *et al*., 1993). PE metabolism has been studied mainly in respect to its role in the biogenesis of the glycosylphosphatidylinositol anchor used for membrane attachment of important surface proteins, such as the variant surface glycoprotein (Rifkin and Fairlamb, 1985; Rifkin *et al*., 1995). Bloodstream and procyclic forms of *T. brucei* differ in phospholipid subclass and molecular species composition (Dixon and Williamson, 1970; Patnaik *et al*., 1993; van Hellemond and Tielens, 2006), but little is known about the lipid composition and dynamics of organellar membranes, and the consequences of perturbed lipid synthesis. Mutant phenotypes attributed to changes in lipid composition include alterations in mitochondrial morphology and inhibition of respiration following RNAi knock-down of the mitochondrial acyl carrier protein (ACP) (Guler *et al*., 2008) and the cytokinesis defects following RNAi knock-down of serine palmitoyltransferase, an essential enzyme in sphingolipid biosynthesis (Fridberg *et al*., 2008).

We have recently elucidated the complete pathway for PE synthesis in *T. brucei* procyclic forms and demonstrated that *de novo* PE synthesis depends exclusively on the Kennedy pathway (Signorell *et al*., 2008a) (Fig. 1). In the present report, we use RNAi to knock down the Kennedy pathway enzymes ethanolamine kinase (EK), ethanolamine-phosphate cytidylyltransferase (ET), ethanolamine phosphotransferase (EPT) and choline-/ethanolamine phosphotransferase (CEPT) to study in more detail the cellular and morphological consequences of altered phospholipid composition in *T. brucei* procyclic forms. By careful analysis of early-onset phenotypes, we discovered that the most immediate effect of an RNAi-mediated depletion of ET was a change of mitochondrial morphology and perturbation of the inner mitochondrial membrane topology. In contrast, RNAi knock-down of CEPT resulted in a specific cell division phenotype with production of anucleate zoids.

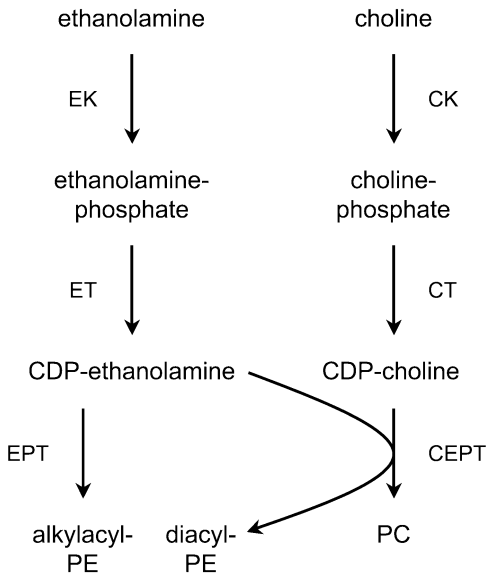

Fig. 1. Biosynthesis of PE and PC in *T. brucei* procyclic forms. Schematic representation of the CDP-ethanolamine and CDP-choline branches of the Kennedy pathway (adapted from Signorell *et al*., 2008a). EK, ethanolamine kinase, Tb11.18.0017; CK, choline kinase, Tb927.5.1140; ET, ethanolamine-phosphate cytidylyltransferase, Tb11.01.5730; CT, choline-phosphate cytidylyltransferase, Tb10.389.0730; EPT, ethanolamine phosphotransferase, Tb10.389.0140; CEPT, choline-/ethanolamine phosphotransferase, Tb10.6k15.1570. In this study, the expression of EK, ET, EPT and CEPT was downregulated by RNAi.

Results

Onset of phenotype

We have previously reported a detailed phospholipid analysis of *T. brucei* procyclic forms after 5 days of induction of RNAi against EK, ET, EPT and CEPT (Signorell *et al*., 2008a,b). These compositional analyses represented values for whole cells after depletion of the respective enzymes after extended incubation times and, thus, may have missed possible transient changes, or specific or preferential effects on particular organelles. To study this we have extended our biochemical analyses and complemented them with a detailed characterization of the cellular phenotypic consequences of lipid modulation. Cell-cycle progression and DNA content were analysed by microscopy-based approaches and flow cytometry, whereas mitochondrial morphology and activity were studied by immunofluorescence microscopy and MitoTracker staining, combined with measurement of mitochondrial ATP production. Finally, an electron microscopic approach was used to visualize specific organelle impairment.

To obtain detailed information on the RNAi-mediated phospholipid changes over time, we measured the total phospholipid composition of all four *T. brucei* RNAi mutants, EK, ET, EPT and CEPT, at 24 h intervals during the first 5 days of induction, using two-dimensional thin-layer chromatography (TLC) and lipid phosphorus determination. Knock-down of EK, ET and EPT resulted in a progressive decrease of the PE to PC ratio during the first 3 days of induction and thereafter reached a plateau at 0.21 for EK and 0.07 for ET RNAi cells (Fig. 2). These

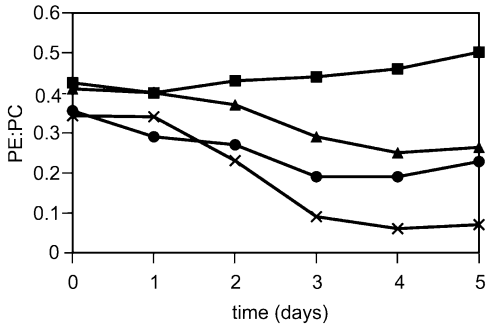

Fig. 2. Effects of RNAi-mediated knock-down of PE biosynthetic enzymes on phospholipid composition. (A) Parasites were cultured in the presence of tetracycline for the indicated times, and lipids were extracted from 4×10^8 trypanosomes using organic solvents. After separation by two-dimensional TLC, all major lipid spots were scraped from the plates and quantified by phosphorus analysis. The data represent the ratios of PE to PC after downregulation of EK (circles), ET (crosses), EPT (triangles) and CEPT (squares). The PE to PC ratios in uninduced cells remained constant (data not shown).

results are consistent with our previous findings that downregulation of ET for 5 days causes a more severe drop in PE than RNAi against EK (Signorell *et al*., 2008a). A decrease in the PE to PC ratio to 0.23 was also observed during downregulation of EPT (Fig. 2); however, as previously shown, this was not due to a drop in PE but rather an increase in PC (Signorell *et al*., 2008a). In contrast, the ratio of PE to PC increased slightly to 0.44 during RNAi against CEPT (Fig. 2), which is consistent with the previously observed decrease of the PC content in CEPT RNAi cells after 5 days of induction (Signorell *et al*., 2008a). The relative amounts of the other phospholipid classes, phosphatidylserine (PS), phosphatidylinositol, inositolphosphoceramide, sphingomyelin and cardiolipin, remained unchanged during the entire time-course of RNAi against all four PE biosynthetic enzymes (results not shown), except that PS dropped to almost undetectable levels after 5 days of downregulation of ET (see also Signorell *et al*., 2008a).

All RNAi mutants grew normally during the first 3 days of RNAi induction, but stopped dividing thereafter, with the RNAi knock-down of ET causing the strongest effect on growth rate (Fig. S1; Signorell *et al*., 2008a).

RNAi against ET affects mitochondrial morphology

To study possible effects of an altered phospholipid composition on membrane and organelle integrity, we analysed parasites after RNAi against all four PE biosynthetic enzymes by fluorescence and electron microscopy. Using MitoTracker as a marker for mitochondria, we observed a pronounced change in the morphology of the mitochondrion following RNAi knock-down of ET (Fig. 3A–E). MitoTracker staining of the uninduced control cells shows the characteristic tubular structure of the single mitochondrion (Fig. 3A and B). Starting at 3–4 days post induction, an increasing number of parasites showed a less complex tubular pattern and, at 5–6 days post induction, the MitoTracker-positive areas in all cells were reduced to a few discrete spots (Fig. 3C–E). Because MitoTracker staining depends on a mitochondrial membrane potential, antibody labelling of heat-shock protein 60 (Hsp60) was used as an alternative probe to examine mitochondrial morphology, and this produced a staining pattern similar to MitoTracker (Fig. 3F).

Further examination of cellular ultrastructure by transmission electron microscopy (TEM) clearly showed abnormal mitochondrial morphology in ET RNAi cells (Fig. 4). The most obvious difference between control and ET-depleted cells was a time-dependent disappearance of normally shaped cristae (Fig. 4A–D). After 5 days of RNAi, the mitochondrion was essentially devoid of the plate-like cristae characteristic of the procyclic-form mitochondrion. Instead, numerous intramitochondrial vesicular structures accumulated (Fig. 4B–D, indicated by the white arrows). In addition, the region of the mitochondrion harbouring the kinetoplast DNA appeared dilated (compare Fig. 4A with Fig. 4B–D). However, ET RNAi had no obvious effect on the structure of the kinetoplast DNA disk itself, nor did it affect its close association with the mitochondrial membrane near the base of the flagellum. Interestingly, with increasing induction time the mitochondrial matrix appeared more electron dense, suggesting changes in matrix structure and/or composition. In addition, in most cells showing abnormal mitochondrial morphology, we noticed the appearance of a gap between the two membranes of the nuclear envelope (Fig. 4D, indicated by the black arrow).

In contrast to the results obtained with ET RNAi cells, trypanosomes depleted of EK, EPT or CEPT using RNAi showed normal mitochondrial structure as assessed by TEM, MitoTracker staining and labelling of Hsp60 (data not shown).

Furthermore, examination of membranes in the different RNAi cells by TEM showed no obvious morphological abnormalities in the Golgi cisternae, endoplasmic reticulum, flagellar pocket or plasma membranes (data not shown).

Mitochondria in ET RNAi cells maintain ATP production

Staining of mitochondria with MitoTracker depends on an intact mitochondrial membrane potential. To confirm that after downregulation of ET the mitochondria maintain production of ATP by oxidative phosphorylation, we measured ATP generation in isolated mitochondria using succinate as substrate (Bochud-Allemann and Schneider,

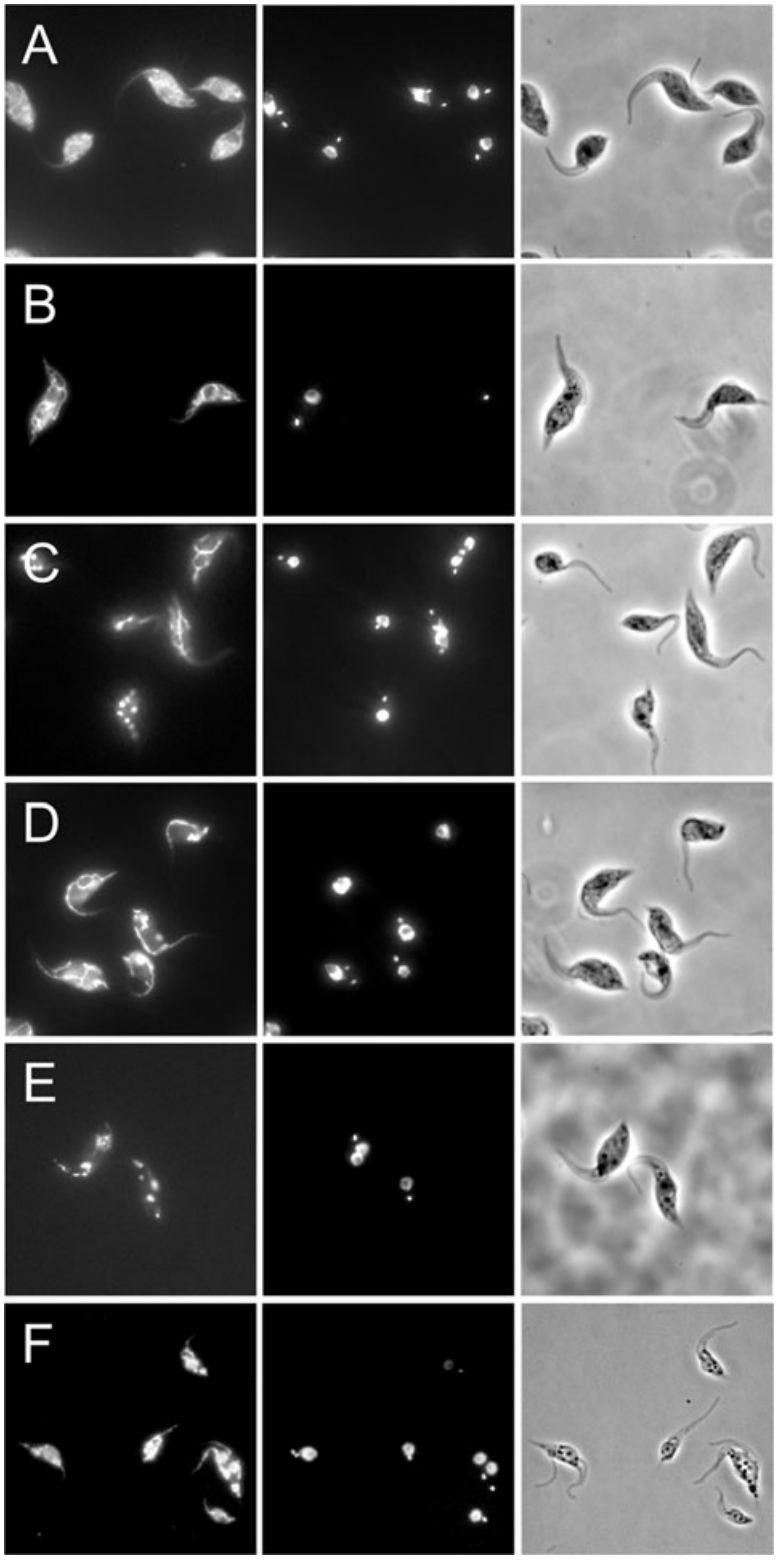

Fig. 3. Changes in mitochondrial morphology following RNAi knock-down of ET. Trypanosomes were grown in the presence of tetracycline for 0 (A), 3 (B), 4 (C), 5 (D, F) or 6 (E) days. The left panels show mitochondria labelled with MitoTracker (A–E), or with an antibody against the mitochondrial matrix protein Hsp60 (F). The central panels show DNA stained with DAPI, and the right panels show a phase-contrast image of the cells.

2002). In addition, we determined ATP production by substrate-level phosphorylation using α-ketoglutarate as substrate (Bochud-Allemann and Schneider, 2002). The results in Fig. 5 show that mitochondrial ATP production by either pathway was unchanged in trypanosomes after RNAi-mediated knock-down of ET. In control experiments, ATP production was blocked by the addition of the ADP/ATP translocation inhibitor, atractyloside, demonstrating

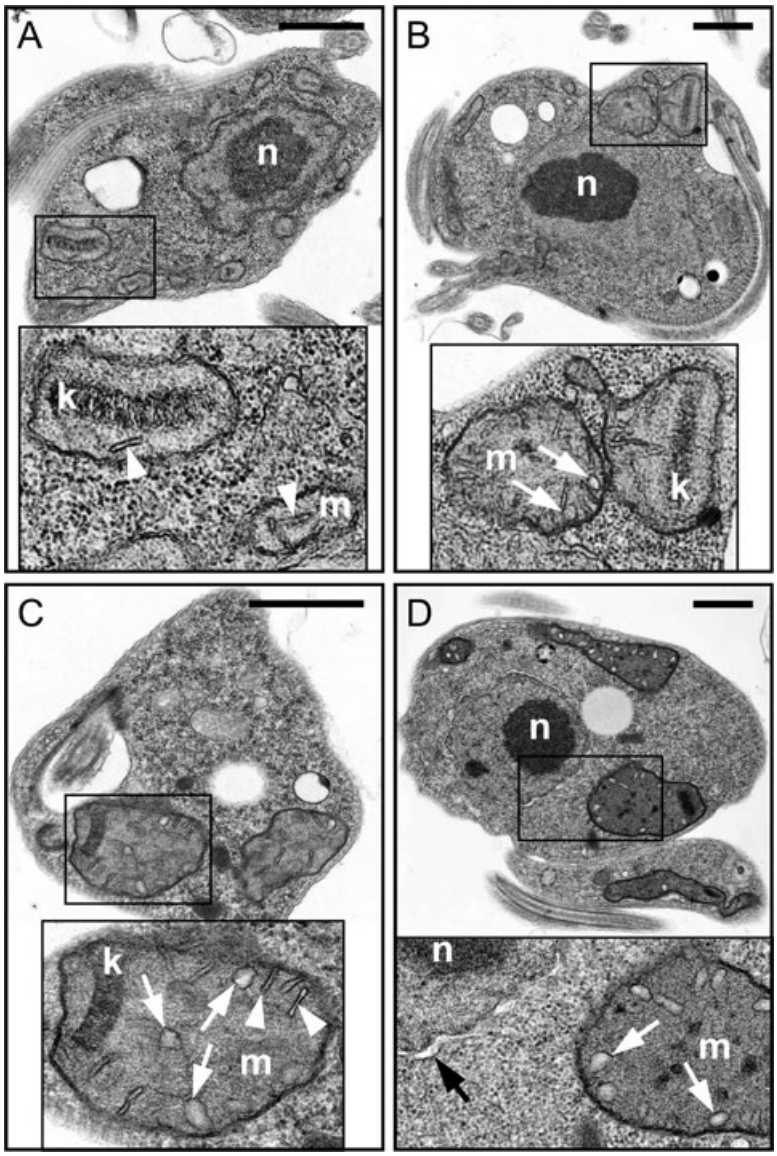

Fig. 4. Changes in mitochondrial ultrastructure following RNAi against ET. Trypanosomes were grown in the presence of tetracycline for 0 (A), 3 (B), 4 (C) or 5 (D) days and processed for TEM. The insets show enlarged views of mitochondrial profiles (m) and kinetoplasts (k). Ultrastructural changes were observed in the inner mitochondrial membrane. Examples of normal disk-like cristae are indicated with arrowheads. Following induction of ET RNAi, vesicular structures were observed (white arrows). A distended nuclear envelope (black arrow) was seen in some cells 5 days after induction of RNAi; n, nucleus. Calibration bars, 1 μm.

that ATP was indeed generated in the mitochondrion. Together, the data indicate that, although the mitochondrial structure was altered and the organelle looked fragmented as assessed by light microscopy, it remained functional in terms of energy production.

ET RNAi affects cell shape

In addition to the effects on mitochondrial morphology, RNAi knock-down of ET also resulted in distinct alterations of cell shape, as revealed by scanning electron microscopy (SEM) (Fig. 6). Many cells (up to 12% of the population) had a strikingly elongated posterior end. Typical examples of such trypanosomes viewed by SEM are shown in Fig. 6B and C. The proportion of these cells in the population increased steadily following RNAi induction without reaching a plateau (Fig. 6E). The majority of elongated cells were at the 1K1N (one kinetoplast, one nucleus) stage of the cell cycle but the proportion of 2K1N, 2K2N and 1K2N cells with elongated posterior ends increased over time from 18.8% to 35.8% of total cells between day 5 and 8 of induction (Fig. 6F). We also observed cell pairs that had elongated posterior ends which remained connected by long membrane bridges (Fig. 6D, indicated by the arrow head), possibly indicating a defect in the late stage of cytokinesis.

Interference with the Kennedy pathway impairs normal cell-cycle progression

To investigate the effect of the altered phospholipid composition on cell-cycle progression and cytokinesis further,

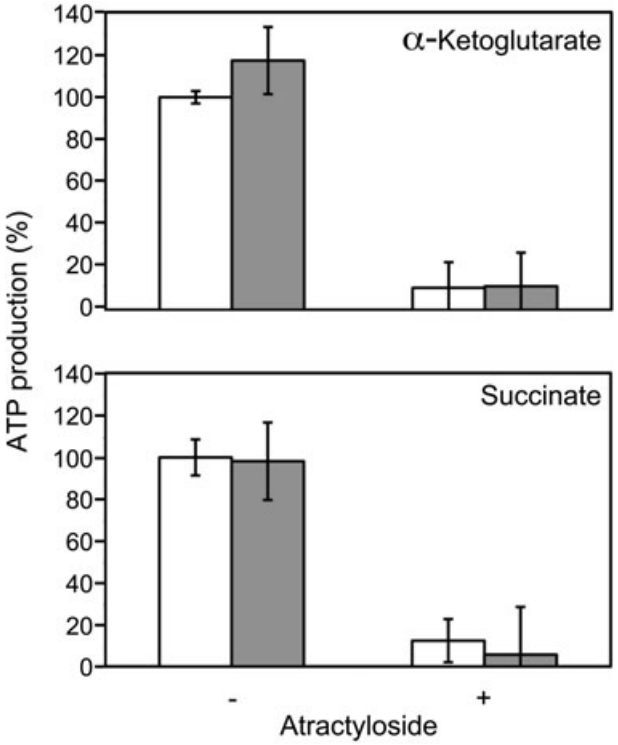

Fig. 5. Mitochondrial ATP production after RNAi against ET. Mitochondria were isolated from equal numbers of trypanosomes after 5 days of culture in the absence (white bars) or presence (grey bars) of tetracycline using digitonin. Substrate-level phosphorylation was measured by addition of α-ketoglutarate as substrate. Oxidative phosphorylation was measured with succinate as substrate. To control for mitochondrial ATP production, the translocation of ADP/ATP across the inner mitochondrial membrane was inhibited by the addition of atractyloside to the reaction. The data represent mean values ± standard deviations from three experiments.

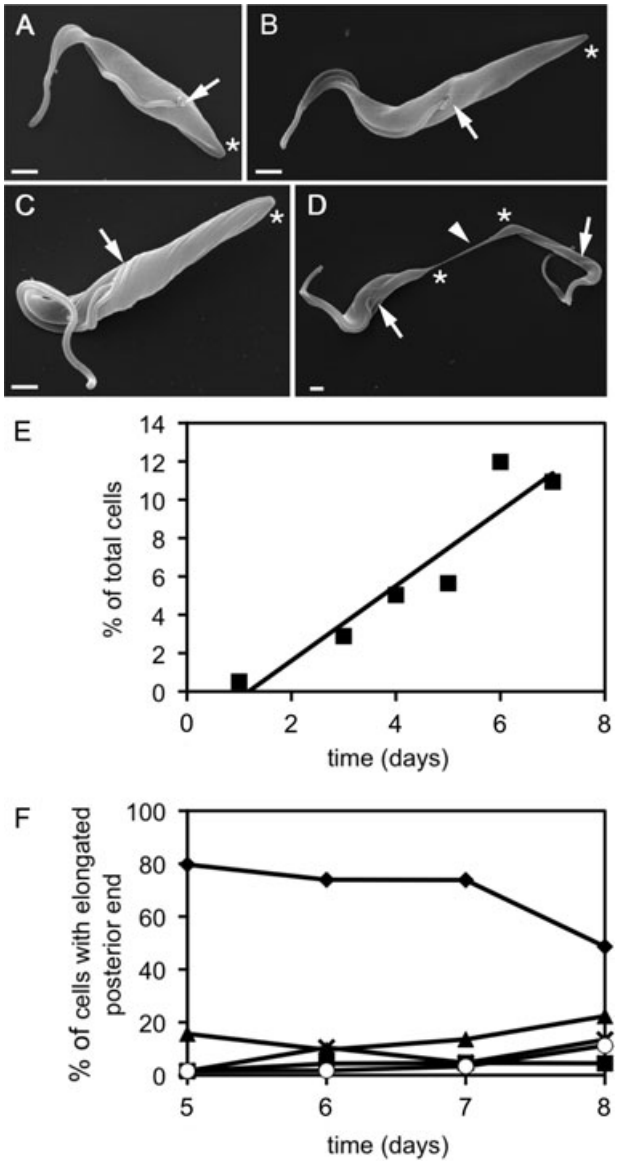

Fig. 6. Changes in cell shape following RNAi against ET.
A–D. Trypanosomes were grown in the presence of tetracycline for 0 (A), 3 (B), 4 (C) or 5 (D) days and processed for SEM. The posterior end of the cell is indicated by an asterisk, and the area where the flagellum exits the flagellar pocket, by an arrow. The arrowhead indicates a connection between two elongated cells. Calibration bars, 1 μm.
E. Trypanosomes with an elongated posterior end (defined by a > 50% increase in length) were quantified by counting at least 500 cells from three separate experiments and plotted as a percentage of the total cell population. A linear trend line was fitted.
F. Trypanosomes with an elongated posterior end were analysed for their position in the cell cycle. Cells induced for ET RNAi for 5–8 days were fixed and stained with DAPI as described in Fig. 3. At each time point, the numbers of kinetoplasts (K) and nuclei (N) were counted in 64–179 cells with elongated posterior end and the frequency of each category was plotted as the percentage of the total cell population. 1K1N (diamonds), 2K1N (squares), 2K2N (triangles), 1K2N (crosses), cells with > 2K and > 2N (circles).

we analysed nuclei and kinetoplast distribution in cells for 8 days after induction of RNAi against EK, ET, EPT and CEPT. Depletion of ET or EPT resulted in a decrease in the number of parasites with one kinetoplast and one nucleus (1K1N; from 80% to < 40%; Fig. 7A), while the number of cells with multiple kinetoplasts and nuclei increased from < 1% to 24–30% (Fig. 7A), indicating that a large proportion of cells in the population failed to complete cytokinesis but progressed to another round of organelle duplication. In addition, we found that knockdown of ET caused a > 10-fold increase in the number of anucleate 1K0N cells (zoids) from < 0.5% to 5–8% (Fig. 7A). A similar increase in 1K2N cells (from < 0.5% to 8–9%) suggests that a subpopulation of cells underwent an asymmetric cell division where a 2K2N cell divided incorrectly to produce one zoid and one 1K2N daughter cell. Downregulation of EK had little effect on the number and distribution of kinetoplasts and nuclei (Fig. 7A).

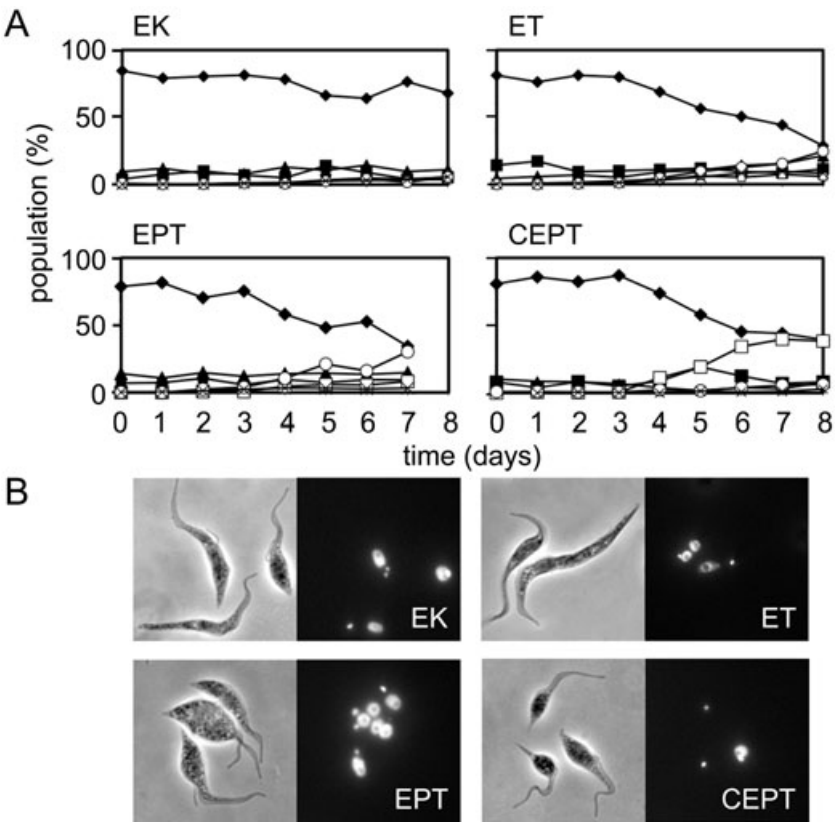

Fig. 7. Effects of RNAi against PE biosynthetic enzymes on cell-cycle progression and morphology.
A. Trypanosomes were cultured in the presence of tetracycline to induce RNAi for 7–8 days, fixed, and DNA was stained with DAPI. At each time point, the numbers of kinetoplasts (K) and nuclei (N) were counted in at least 500 cells after downregulation of EK, ET, EPT and CEPT. The frequency of each category was plotted as the percentage of the total cell population. 1K1N (diamonds), 2K1N (filled squares), 2K2N (triangles), 1K0N (open squares), 1K2N (crosses), cells with > 2K and > 2N (circles).
B. Trypanosomes were fixed 6 days after RNAi induction and stained with DAPI. Individual composites show representative phase-contrast images (left) and DNA staining (right) of cells after knock-down of EK, ET, EPT and CEPT.

CEPT RNAi results in production of zoids

RNAi knock-down of CEPT resulted in a dramatic increase in 1K0N cells from 0.5% to > 38%, accompanied by a decrease in the number of 1K1N cells from > 80% to 40% (Fig. 7A). A rise in the number of 1K2N cells was not observed following CEPT RNAi. The KN profile of CEPT RNAi cells suggested that cells were undergoing cytokinesis in the absence of nuclear division, resulting in the production of one anucleate zoid and one 1K1N cell. These cells were further examined by flow cytometry to measure DNA content (Fig. 8A). On day 7, 37% of the cells in the population had a DNA content of < 1C (Fig. 8B). This subpopulation, which first appeared on day 3 and increased sharply thereafter, likely represents the zoids. The proportion of cells with 2C DNA content sharply decreased between days 3 and 5 after induction (Fig. 8), which correlates with the decrease of 1K1N cells from day 3 (Fig. 7A). In addition, we noticed an increasing proportion of cells with 8C DNA content (15% on day 7) (Fig. 8). Such increased DNA content is a feature either of cells that contain more nuclei than normal, or of cells that re-initiated nuclear S-phase without having gone through mitosis. The latter scenario is more likely for CEPT RNAi cells, because the analysis of DAPI-stained cells showed no accumulation of multinucleate (> 2N) cells (Fig. 7A). Taken together, the data suggest that as a consequence of CEPT knock-down, nuclear division fails, but DNA replication continues and the cells proceed with cytokinesis.

Discussion

Changes in the membrane lipid composition are expected to have major pleiotropic effects on a cell. Here, we analysed the distinct phenotypes resulting from RNAi-mediated knock-down of enzymes of the Kennedy pathway for PE synthesis in *T. brucei* procyclic forms. Mitochondrial morphology was severely altered by RNAi knock-down of ET, which causes the strongest reduction in PE. In contrast, RNAi knock-down of CEPT, which affects primarily PC synthesis, resulted in a nuclear division phenotype and the generation of anucleate zoids. These results reveal which organelles or processes are most sensitive to a perturbation of normal levels of the major phospholipids in *T. brucei*.

The earliest, and most striking effect of ET RNAi is seen in the mitochondrion. This mitochondrial phenotype was characterized by an increased electron density, alteration of inner mitochondrial membrane morphology, affecting cristae, and loss of the branched tubular network morphology. Following ET RNAi, we observed a reduction in the number of normal plate-like cristae accompanied by the appearance of vesicular structures. The most parsi-

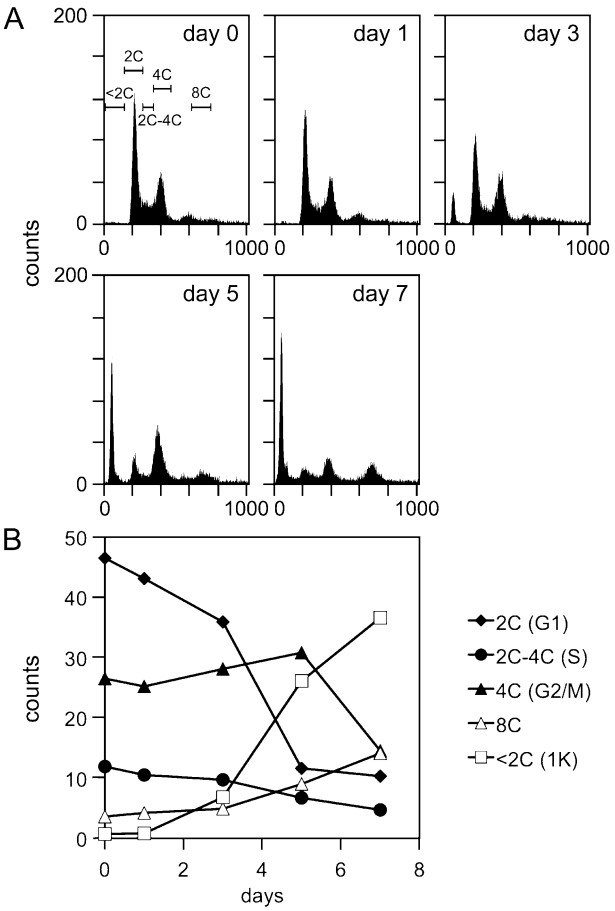

Fig. 8. Flow cytometric analysis of DNA contents in CEPT RNAi cells.
A. CEPT RNAi was induced for 0–7 days as indicated. At each time point, cells were stained with propidium iodide and subjected to FACS analysis. Each histogram represents 10 000 events.
B. The data from (A) showing trypanosomes with 2C, 2–4C, 4C, 8C and < 2C DNA content were plotted relative to the total cell population. The gates used for quantification are shown in (A).

monious explanation is that these membrane bounded structures originated from the cristae. However, the precise relationship between these vesicular structures and the inner mitochondrial membrane, and whether there was continuity between them, could not be determined with certainty. ET RNAi caused the sharpest reduction of total levels of PE, and resulted in a decrease of PS, without affecting the cellular levels of PC (see also Signorell *et al*., 2008a). A reduction of PE (and PS) levels in subdomains of the mitochondrion may directly affect the curvature of the membrane and its ability to form and maintain normally shaped cristae. Alternatively, the distribution of membrane proteins may have been affected by changes in lipid composition causing disruption of normal membrane topology. Although we cannot distinguish between these possibilities, the specific alterations of mitochondrial structure early after induction of ET RNAi provide further evidence that the inner mitochondrial membrane of procyclic *T. brucei* is highly sensitive to a perturbation of phospholipid metabolism. A similar observation was made in a recent study about the effects of RNAi knock-down of ACP in procyclic-form trypanosomes (Guler *et al*., 2008). ACP RNAi affected the structure of the mitochondrion and reduced oxygen consumption, indicating that respiration had been inhibited. Changes in lipid composition, a decrease of diacyl-PE and phosphatidylinositol in the mitochondrion, were thought to be the primary cause of disrupted mitochondrial function because they preceded the other phenotypes. In the present study, cells induced for ET RNAi continued to produce ATP, indicating that the electron transport chain remained fully functional in these cells, despite the ultrastructural changes. Concentration of MitoTracker staining to discrete foci indicates that energetically active areas of the mitochondrion were dispersed. Whether the mitochondrion is physically fragmented could not be determined with certainty.

Following ET RNAi, the mitochondrial profiles observed in the TEM appear more electron dense than in the uninduced cells. The opposite effect, i.e. a reduction in electron density in the mitochondrion, has been reported after RNAi knock-down of ACP (Guler *et al*., 2008). In preparation for TEM, cells in both studies were post-fixed with osmium tetroxide, which reacts with lipid moieties, thereby adding density to the biological material. In the ACP RNAi cells, the reduced electron density may reflect a decrease in lipid content. In the ET RNAi cells, the mitochondrial matrix appears more osmophilic, which may indicate a local increase in lipid content.

The precise three-dimensional topology of inner mitochondrial membranes in general has remained controversial and theoretical models as to how the cristae structure might be determined at the molecular level have recently been reviewed (Zick *et al*., 2009). Electron tomography of rat liver mitochondria has started to provide new insights into mitochondrial structure and dynamics, by producing high-resolution models of the mitochondrial membrane architecture and describing the tubular junctions between cristae and inner mitochondrial membrane under different conditions (Frey and Mannella, 2000; Mannella, 2006; 2008). Dissecting the mechanisms that govern the normal morphological changes in the trypanosome mitochondrion, such as the correlation of cristae development with a respiratory switch to oxidative metabolism, might uncover important general principles of mitochondrial biology.

In addition to the mitochondrial phenotype, knock-down of ET RNAi led to the accumulation of 20% of cells with > 2 kinetoplasts and > 2 nuclei, suggesting that these cells had failed to go through cytokinesis. Moreover, some cells remained connected at their posterior ends by membrane

bridges, indicating a block or delay in the late stage of cytokinesis. While PE is predominantly found on the cytoplasmic side of cellular membranes, studies of mammalian cells have shown that re-distribution to the surface of the cleavage furrow is necessary for cytokinesis, and mutant Chinese hamster ovary cells with decreased PE levels exhibited a defect in late cytokinesis, which was attributed to a defect in contractile ring disassembly (Emoto and Umeda, 2000; Emoto *et al*., 2005). Interestingly, a mutant strain of *Escherichia coli* deficient in PE is also blocked in cytokinesis (Rietveld *et al*., 1997). This *E. coli* strain shows an absolute dependence on divalent cations for normal growth (DeChavigny *et al*., 1991). Since divalent cations are known to induce non-bilayer-phase formation in cardiolipin model membranes, the lack of the non-bilayer lipid PE in mutant *E. coli* may directly be responsible for a block in cytokinesis (Rietveld *et al*., 1993; 1997). Non-bilayer lipids have been implicated in processes such as membrane fusion, transbilayer movement of lipids and membrane protein function (Siegel and Epand, 1997; van den Brink-van der Laan *et al*., 2004; Epand, 2007). Similarly, in *T. brucei*, a lack of PE may directly affect cytokinesis by preventing membrane fusion events late in cytokinesis, resulting in trypanosome pairs still connected by long membrane bridges and unable to completely separate. However, a direct role for PE, if any, in the formation of the cleavage furrow, furrow ingression or abscission in *T. brucei* remains to be determined.

Alternatively, since division of the complex *T. brucei* mitochondrion is intimately linked with division of other organelles and a mitochondrial activation has been proposed to play a determining role in the morphogenesis of the procyclic form (Vickerman, 1965), disruption of the mitochondrial structure could have downstream effects and possibly interfere with cytokinesis and cell morphogenesis.

Superficially, the morphological phenotype observed in the ET RNAi cells bears some resemblance to the nozzle phenotype defined before (Hendriks *et al*., 2001), which is caused by a polar extension of microtubules at the posterior end of procyclic *T. brucei*, resulting in a specific increase of the distance from the kinetoplast to the posterior end in 1K1N cells. However, in contrast to the nozzle phenotype defined by Hendriks *et al*. (2001), and subsequently by Hammarton *et al*. (2004), we found no evidence of a G1/S block in the ET RNAi cells with 'nozzle-like' morphology.

RNAi knock-down of CEPT produced a cell division phenotype characterized by accumulation of zoids. Similarly high proportions of zoids have previously been observed in *T. brucei* procyclic forms under conditions where mitosis was blocked, for example, by pharmacological inhibitors (Robinson *et al*., 1995; Ploubidou *et al*., 1999), RNAi knock-down of the mitotic cyclin CYC6 (Hammarton *et al*., 2003) and expression of a Separase-resistant cohesin subunit SCC1 (Gluenz *et al*., 2008). Zoids also accumulated under conditions where segregation of post-mitotic nuclei was aberrant, following for example treatment with the antimicrotubule agent rhizoxin (Ploubidou *et al*., 1999) or RNAi knock-down of centrin 4 (Shi *et al*., 2008). Flow cytometry and cytology suggested that CEPT RNAi inhibited nuclear division. Our data are consistent with a model where the first division of the affected cells produces one zoid and one 1K1N* [4C DNA content (Ploubidou *et al*., 1999)] daughter cell. The 1K1N* cell then re-initiates a further round of organelle duplication and at cell division produces another zoid and a 1K1N** (8C DNA content) daughter cell. PC has previously been associated with mitosis in mammalian cells. HeLa cells increase levels of PC synthesis in late mitosis and the newly synthesized PC is predominantly incorporated into nuclear envelope membrane as it re-forms during telophase (Henry and Hodge, 1983). The orthologue of CEPT in other organisms has been localized to the ER and nuclear envelope membrane (Henneberry *et al*., 2002). Association of newly synthesized PC with the nuclear envelope membrane is therefore not necessarily restricted to re-formation of a nuclear membrane after completion of mitosis but might also occur in cells that undergo a closed mitosis, such as *T. brucei*. Trypanosomes probably co-ordinate membrane phospholipid synthesis with the cell cycle, analogous to mammalian cells (Jackowski, 1994; Banchio *et al*., 2003), but this has not been demonstrated experimentally. CEPT was the only enzyme, of the four examined in the present study, where RNAi resulted in a decrease of PC (to 64% of wild-type levels; see also Signorell *et al*., 2008a). Regulation of nuclear division in procyclic *T. brucei* may thus depend on new PC synthesis, or possibly PC levels remaining above a threshold level. Interestingly, the knock-down of EPT caused a strong increase in PC (see also Signorell *et al*., 2008a) and resulted in an increase in the number of cells with > 2 kinetoplasts and > 2 nuclei from 0% on day 3 to 30% on day 7 after RNAi induction. This shows that elevated levels of PC had no inhibitory effect on nuclear division, but cytokinesis was impaired, possibly due to a lack of PE.

In summary, we conclude that in *T. brucei* procyclic forms the mitochondrial structure, particularly the inner mitochondrial membrane, is most sensitive to a depletion of PE levels (ET RNAi), while nuclear division is affected by a decrease in the PC content (CEPT RNAi).

Experimental procedures

Unless otherwise specified, all reagents were of analytical grade and were from Merck (Darmstadt, Germany), Sigma-Aldrich (Buchs, Switzerland) or MP Biomedicals (Tägerig,

Switzerland). All EM supplies were from Agar Scientific (Stansted, UK) or TAAB Laboratories (Reading, UK).

Trypanosomes and culture conditions

The following gene products were downregulated by RNAi using stem-loop constructs containing a puromycin resistance gene: *T. brucei* EK (GeneDB Accession No. Tb11.18.0017), *T. brucei* ET (Tb11.01.5730), *T. brucei* CEPT (Tb10.6k15.1570) and *T. brucei* EPT (Tb10.389.0140). Details on the construction of the RNAi cell lines and on trypanosome culture conditions are provided elsewhere (Signorell *et al*., 2008a,b).

Analysis of nucleus and kinetoplast configurations

Cell densities and approximate cell volumes were determined daily using a Casy TT cell counter (Schärfe System, Reutlingen, Germany) or a Neubauer counting chamber. The cell density was kept between 3×10^6 cells ml^{-1} and 1.5×10^7 cells ml^{-1} during all experiments. Antibiotics were omitted during the course of the entire experiment, except for the addition of tetracycline. At a given time point, parasites were washed twice with phosphate-buffered saline (PBS; 137 mM NaCl, 2.6 mM KCl, 8 mM Na_2HPO_4, 1.5 mM KH_2PO_4, pH 7.2) and allowed to settle onto glass microscope slides (Erie Scientific Company, Portsmouth, NH). Trypanosomes were fixed with –20°C methanol for at least 10 min and subsequently washed twice with PBS. The slides were mounted using Vectashield containing 4′,6′-diamidino-2-phenylindol (Dapi; Vector Laboratories, Burlingame, CA) to visualize nuclear and mitochondrial DNA. Counts of nuclei (N) and kinetoplasts (K) were performed on a Leica Leitz DM RBE microscope and on a Nikon Eclipse TE2000-E microscope. Nucleus and kinetoplast configurations were assessed from the entire cell population (at least 500 cells per time point), or from the subpopulation of cells with an elongated posterior end (64–179 per time point). Light microscopy pictures were made using the Leica Leitz DM RBE microscope equipped with a Photometrics CoolSNAP fx camera.

Electron microscopy

For TEM, parasites were fixed for 5 min with 2.5% glutaraldehyde in culture medium before being transferred to buffered fixative (2.5% glutaraldehyde, 2% paraformaldehyde, 0.1% picric acid in 100 mM phosphate buffer, pH 7.0) for 2–24 h. The fixed cells were washed with 200 mM phosphate buffer, pH 7.0, and post-fixation was performed with 1% osmium tetroxide in 100 mM phosphate buffer, pH 7.0, for 1.5 h at 4°C. After thorough washing with water, fixed cells were stained *en bloc* with 2% aqueous uranyl acetate for 2 h at 4°C in the dark, rinsed with water, dehydrated with ascending acetone concentrations and embedded in epon resin. Sections of 60–70 nm were analysed with a Philips Tecnai 12 transmission electron microscope.

For SEM, parasites were fixed in 2.5% glutaraldehyde in culture medium for 2 h, washed and re-suspended in PBS at a density of 2–4 $\times 10^7$ cells ml^{-1}. Cells were allowed to settle onto 13-mm-diameter coverslips (Chance Propper, Smethwick, UK), rinsed with water and dehydrated with ascending ethanol concentrations. Samples were critical-point dried and coated with gold. Specimens were analysed with a Jeol JSM-5510 scanning electron microscope.

Immunocytochemistry

For staining of mitochondria, 1×10^7 parasites were incubated with 0.1 μM MitoTracker Red CMXRos (Invitrogen, Basel, Switzerland) in culture medium for 15 min at 27°C, washed twice with PBS and left to settle onto glass microscope slides. Cells were fixed with 4% formaldehyde in PBS for 10 min, permeabilized with 0.1% NP40 in PBS for 5 min and washed three times with PBS. DNA was visualized by incubation with 5 μg ml^{-1} Dapi for 1 min. Fixed cells were washed three times with PBS and mounted with 1% 1,4-diazabicyclo[2.2.2]octan, 90% glycerol in 50 mM sodium phosphate buffer, pH 8.0. Samples were analysed using a Leica Leitz DM RBE microscope equipped with a Photometrics CoolSNAP fx camera.

Immunofluorescence labelling of the mitochondrial matrix was performed as follows: trypanosomes were washed once with serum-free SDM-79 and allowed to settle onto glass microscope slides (Erie Scientific Company, Portsmouth, NH). Parasites were fixed with 4% paraformaldehyde in PBS for 10 min. Mouse polyclonal antiserum against mitochondrial matrix Hsp60 was used at a dilution of 1:100 in PBS for 1 h at room temperature. Subsequently, cells were washed three times with PBS and incubated with secondary antibody Alexa Fluor 568 goat anti-mouse IgG (Invitrogen, Basel, Switzerland) at a dilution of 1:1000 for 1 h at room temperature. Slides were washed three times with PBS and mounted using Vectashield. Fluorescence microscopy was performed on a Nikon Eclipse E600 microscope equipped with a Nikon Digital Camera DXM 1200 and the RCT-1® software provided by the manufacturer.

Fluorescence-activated cell sorting (FACS)

Trypanosomes (2×10^7) cells were fixed in 0.25% formaldehyde for 5 min at room temperature and subsequently in 10 volumes of ice-cold 70% ethanol for 30 min on ice. Cells were examined by light microscopy to confirm that no clumping had occurred. Cells were re-suspended in 4 ml of PBS containing 40 μg ml^{-1} propidium iodide and 10 μg ml^{-1} RNase A and incubated at 37°C for 30 min. The DNA content of propidium iodide-stained cells was analysed with a FACSCalibur analytical flow cytometer (Becton Dickinson, Oxford, UK) with a HeNe laser (excitation wavelength 488 nm). The percentages of cells with DNA content < 2C, 2C, 2–4C, 4C and 8C were determined using the CellQuest Pro software version 6.0 (Becton Dickinson). Gates for the different cell phases/populations were set manually. For each time point, 10 000 events were measured.

Lipid extraction and phosphorous determination

Trypanosome lipids were extracted with chloroform : methanol (2:1, by volume) as described before (Signorell *et al*., 2008a). Phospholipids were separated by two-dimensional

TLC using solvent system 1 (chloroform : methanol : ammonia : water, 90:74:12:8, by volume) for the first and solvent system 2 (chlorofom : methanol : acetone : acetic acid : water, 40:15:15:12:8, by volume) for the second dimension (Bütikofer *et al.*, 1989). On each plate, appropriate lipid standards were run alongside the samples to be analysed. Lipid spots were visualized by exposing the Silica Gel 60 plates to iodine vapour. Phospholids were scraped from the plates and lipid phosphorous was determined as described before (Signorell *et al.*, 2008a).

Isolation of mitochondria and ATP production assay

ATP production was measured in mitochondria isolated from trypanosomes using 0.01% (w/v; final concentration) digitonin exactly as described before (Bochud-Allemann and Schneider, 2002). The isolation of mitochondria from uninduced and induced cells was performed using equal cell numbers as starting material to assure equivalence between the sample preparations. To determine the amount of non-mitochondrial ATP, samples were treated with 6.7 μg ml^{-1} atractyloside for 10 min at 4°C before the ATP assay.

Acknowledgements

We would like to thank Andrew Hemphill, Monika Rauch and Jennifer Jelk for assistance during parts of the project. The work was supported by Swiss National Science Foundation Grant 3100A0-116627 to P.B. and The Wellcome Trust and EP Abraham Trust. K.G. is a Wellcome Trust Principal Research Fellow. P.B. thanks T. Rasmus and M. Bütikofer for valuable input.

References

Banchio, C., Schang, L.M., and Vance, D.E. (2003) Activation of CTP:phosphocholine cytidylyltransferase alpha expression during the S phase of the cell cycle is mediated by the transcription factor Sp1. *J Biol Chem* **278:** 32457–32464.

Bochud-Allemann, N., and Schneider, A. (2002) Mitochondrial substrate level phosphorylation is essential for growth of procyclic *Trypanosoma brucei*. *J Biol Chem* **277:** 32849–32854.

Bogdanov, M., and Dowhan, W. (1999) Lipid-assisted protein folding. *J Biol Chem* **274:** 36827–36830.

Bogdanov, M., Mileykovskaya, E., and Dowhan, W. (2008) Lipids in the assembly of membrane proteins and organization of protein supercomplexes: implications for lipid-linked disorders. *Subcell Biochem* **49:** 197–239.

van den Brink-van der Laan, E., Killian, J.A., and de Kruijff, B. (2004) Nonbilayer lipids affect peripheral and integral membrane proteins via changes in the lateral pressure profile. *Biochim Biophys Acta* **1666:** 275–288.

Brown, R.C., Evans, D.A., and Vickerman, K. (1973) Changes in oxidative metabolism and ultrastructure accompanying differentiation of the mitochondrion in *Trypanosoma brucei*. *Int J Parasitol* **3:** 691–704.

Bütikofer, P., Lin, Z.W., Kuypers, F.A., Scott, M.D., Xu, C., Wagner, G.M., *et al.* (1989) Chlorpromazine inhibits vesiculation, alters phosphoinositide turnover and changes deformability of ATP-depleted RBCs. *Blood* **73:** 1699–1704.

DeChavigny, A., Heacock, P.N., and Dowhan, W. (1991) Sequence and inactivation of the *pss* gene of *Escherichia coli*. Phosphatidylethanolamine may not be essential for cell viability. *J Biol Chem* **266:** 10710.

Dixon, H., and Williamson, J. (1970) The lipid composition of blood and culture forms of *Trypanosoma lewisi* and *Trypanosoma rhodesiense* compared with that of their environment. *Comp Biochem Physiol* **33:** 111–128.

Embley, T.M., and Martin, W. (2006) Eukaryotic evolution, changes and challenges. *Nature* **440:** 623–630.

Emoto, K., and Umeda, M. (2000) An essential role for a membrane lipid in cytokinesis. Regulation of contractile ring disassembly by redistribution of phosphatidylethanolamine. *J Cell Biol* **149:** 1215–1224.

Emoto, K., Inadome, H., Kanaho, Y., Narumiya, S., and Umeda, M. (2005) Local change in phospholipid composition at the cleavage furrow is essential for completion of cytokinesis. *J Biol Chem* **280:** 37901–37907.

Epand, R.M. (2007) Membrane lipid polymorphism: relationship to bilayer properties and protein function. *Methods Mol Biol* **400:** 15–26.

Frey, T.G., and Mannella, C.A. (2000) The internal structure of mitochondria. *Trends Biochem Sci* **25:** 319–324.

Fridberg, A., Olson, C.L., Nakayasu, E.S., Tyler, K.M., Almeida, I.C., and Engman, D.M. (2008) Sphingolipid synthesis is necessary for kinetoplast segregation and cytokinesis in *Trypanosoma brucei*. *J Cell Sci* **121:** 522–535.

Gluenz, E., Sharma, R., Carrington, M., and Gull, K. (2008) Functional characterization of cohesin subunit SCC1 in *Trypanosoma brucei* and dissection of mutant phenotypes in two life cycle stages. *Mol Microbiol* **69:** 666–680.

Guler, J.L., Kriegova, E., Smith, T.K., Lukes, J., and Englund, P.T. (2008) Mitochondrial fatty acid synthesis is required for normal mitochondrial morphology and function in *Trypanosoma brucei*. *Mol Microbiol* **67:** 1125–1142.

Hammarton, T.C., Clark, J., Douglas, F., Boshart, M., and Mottram, J.C. (2003) Stage-specific differences in cell cycle control in *Trypanosoma brucei* revealed by RNA interference of a mitotic cyclin. *J Biol Chem* **278:** 22877–22886.

Hammarton, T.C., Engstler, M., and Mottram, J.C. (2004) The *Trypanosoma brucei* cyclin, CYC2, is required for cell cycle progression through G1 phase and for maintenance of procyclic form cell morphology. *J Biol Chem* **279:** 24757–24764.

van Hellemond, J.J., and Tielens, A.G. (2006) Adaptations in the lipid metabolism of the protozoan parasite *Trypanosoma brucei*. *FEBS Lett* **580:** 5552–5558.

Hendriks, E.F., Robinson, D.R., Hinkins, M., and Matthews, K.R. (2001) A novel CCCH protein which modulates differentiation of *Trypanosoma brucei* to its procyclic form. *EMBO J* **20:** 6700–6711.

Henneberry, A.L., Wright, M.M., and McMaster, C.R. (2002) The major sites of cellular phospholipid synthesis and molecular determinants of fatty acid and lipid head group specificity. *Mol Biol Cell* **13:** 3148–3161.

Henry, S.M., and Hodge, L.D. (1983) Evidence for a unique profile of phosphatidylcholine synthesis in late mitotic cells. *J Cell Biol* **97:** 166–172.

Jackowski, S. (1994) Coordination of membrane phospho-

lipid synthesis with the cell cycle. *J Biol Chem* **269:** 3858–3867.
Jensen, M.O., and Mouritsen, O.G. (2004) Lipids do influence protein function – the hydrophobic matching hypothesis revisited. *Biochim Biophys Acta* **1666:** 205–226.
Lee, A.G. (2004) How lipids affect the activities of integral membrane proteins. *Biochim Biophys Acta* **1666:** 62–87.
Mannella, C.A. (2006) Structure and dynamics of the mitochondrial inner membrane cristae. *Biochim Biophys Acta* **1763:** 542–548.
Mannella, C.A. (2008) Structural diversity of mitochondria: functional implications. *Ann N Y Acad Sci* **1147:** 171–179.
van Meer, G., Voelker, D.R., and Feigenson, G.W. (2008) Membrane lipids: where they are and how they behave. *Nat Rev Mol Cell Biol* **9:** 112–124.
Mileykovskaya, E., Zhang, M., and Dowhan, W. (2005) Cardiolipin in energy transducing membranes. *Biochemistry (Mosc)* **70:** 154–158.
Patnaik, P.K., Field, M.C., Menon, A.K., Cross, G.A.M., Yee, M.C., and Bütikofer, P. (1993) Molecular species analysis of phospholipids from *Trypanosoma brucei* bloodstream and procyclic forms. *Mol Biochem Parasitol* **58:** 97–106.
Ploubidou, A., Robinson, D.R., Docherty, R.C., Ogbadoyi, E.O., and Gull, K. (1999) Evidence for novel cell cycle checkpoints in trypanosomes: kinetoplast segregation and cytokinesis in the absence of mitosis. *J Cell Sci* **112:** 4641–4650.
Rietveld, A.G., Killian, J.A., Dowhan, W., and de Kruijff, B. (1993) Polymorphic regulation of membrane phospholipid composition in *Escherichia coli*. *J Biol Chem* **268:** 12427–12433.
Rietveld, A.G., Verkleij, A.J., and de Kruijff, B. (1997) A freeze-fracture study of the membrane morphology of phosphatidylethanolamine-deficient *Escherichia coli* cells. *Biochim Biophys Acta* **1324:** 263–272.
Rifkin, M.R., and Fairlamb, A.H. (1985) Transport of ethanolamine and its incorporation into the variant surface glycoprotein of bloodstream forms of *Trypanosoma brucei*. *Mol Biochem Parasitol* **15:** 245–256.
Rifkin, M.R., Strobos, C.A.M., and Fairlamb, A.H. (1995) Specificity of ethanolamine transport and its further metabolism in *Trypanosoma brucei*. *J Biol Chem* **270:** 16160–16166.
Robinson, D.R., Sherwin, T., Ploubidou, A., Byard, E.H., and Gull, K. (1995) Microtubule polarity and dynamics in the control of organelle positioning, segregation, and cytokinesis in the trypanosome cell cycle. *J Cell Biol* **128:** 1163–1172.
Schneider, A. (2001) Unique aspects of mitochondrial biogenesis in trypanosomatids. *Int J Parasitol* **31:** 1403–1415.
Shi, J., Franklin, J.B., Yelinek, J.T., Ebersberger, I., Warren, G., and He, C.Y. (2008) Centrin4 coordinates cell and nuclear division in *T. brucei*. *J Cell Sci* **121:** 3062–3070.
Siegel, D.P., and Epand, R.M. (1997) The mechanism of lamellar-to-inverted hexagonal phase transitions in phosphatidylethanolamine: implications for membrane fusion mechanisms. *Biophys J* **73:** 3089–3111.
Signorell, A., Rauch, M., Jelk, J., Ferguson, M.A., and Bütikofer, P. (2008a) Phosphatidylethanolamine in *Trypanosoma brucei* is organized in two separate pools and is synthesized exclusively by the Kennedy pathway. *J Biol Chem* **283:** 23636–23644.
Signorell, A., Jelk, J., Rauch, M., and Bütikofer, P. (2008b) Phosphatidylethanolamine is the precursor of the ethanolamine phosphoglycerol moiety bound to eukaryotic elongation factor 1A. *J Biol Chem* **283:** 20320–20329.
Vickerman, K. (1965) Polymorphism and mitochondrial activity in sleeping sickness trypanosomes. *Nature* **208:** 762–766.
Zick, M., Rabl, R., and Reichert, A.S. (2009) Cristae formation-linking ultrastructure and function of mitochondria. *Biochim Biophys Acta* **1793:** 5–19.

Supporting information

Additional supporting information may be found in the online version of this article.

Please note: Wiley-Blackwell are not responsible for the content or functionality of any supporting materials supplied by the authors. Any queries (other than missing material) should be directed to the corresponding author for the article.

